

# Transverse lattice calculation of the pion light-cone wavefunctions

Simon Dalley

*Department of Physics, University of Wales Swansea  
Singleton Park, Swansea SA2 8PP, United Kingdom*

Brett van de Sande

*Geneva College, 3200 College Ave., Beaver Falls, PA 15010*

## Abstract

We calculate the light-cone wavefunctions of the pion by solving the meson boundstate problem in a coarse transverse lattice gauge theory using DLCQ. A large- $N_c$  approximation is made and the light-cone Hamiltonian expanded in massive dynamical fields at fixed lattice spacing. In contrast to earlier calculations, we include contributions from states containing many gluonic link-fields between the quarks. The Hamiltonian is renormalised by a combination of covariance conditions on boundstates and fitting the physical masses  $\mathcal{M}_\rho$  and  $\mathcal{M}_\pi$ , decay constant  $f_\pi$ , and the string tension  $\sqrt{\sigma}$ . Good covariance is obtained for the lightest  $0^{-+}$  state, which we identify with the pion. Many observables can be deduced from its light-cone wavefunctions. After perturbative evolution, the quark valence structure function is found to be consistent with the experimental structure function deduced from Drell-Yan pi-nucleon data in the valence region  $x > 0.5$ . In addition, the pion distribution amplitude is consistent with the experimental distribution deduced from the  $\pi\gamma^*\gamma$  transition form factor and diffractive dissociation. A new observable we calculate is the probability for quark helicity correlation. We find a 45% probability that the valence-quark helicities are aligned in the pion.

## I. INTRODUCTION

Light-cone wavefunctions encode all of the bound state quark and gluonic properties of hadrons, including their momentum, spin and flavour correlations, in the form of universal process- and frame-independent amplitudes (see, for example, Ref. [1]). Hadronic observables represented as matrix elements of currents are easily expressed in terms of overlaps of light-cone wavefunctions. To compute the wavefunctions, one must diagonalise the light-cone Hamiltonian of QCD in a Fock space of quark and gluonic degrees of freedom. A promising method to achieve this is the transverse lattice formulation of gauge theory [2, 3]. In this approach, the physical gluonic degrees of freedom are represented by gauge-covariant links of colour flux on a lattice transverse to the null-plane of quantisation. In this paper, we set up the method and solve for the light-cone wavefunctions of light mesons using a physically realistic truncation of Fock space on a coarse lattice, spacing  $\sim 2/3$  fm. We obtain good covariance for the light-cone wavefunction of the lightest meson, which we identify with the pion. Results for the pion distribution amplitude (valence quark wavefunction at small transverse separation) and distribution function (valence quark probability at any transverse separation) are consistent with the most recent experimental results in the valence region of light-cone momenta. We find the distribution amplitude to be

$$\phi_\pi(x) = 6x(1-x) \left\{ 1 + 0.15(2) C_2^{3/2}(1-2x) + 0.04(1) C_4^{3/2}(1-2x) \right\} , \quad (1)$$

while the distribution function is

$$V_\pi(x) = \frac{(1-x)^{0.33(2)}}{x^{0.7(1)}} \left\{ 0.33(3) - 1.1(2)\sqrt{x} + 2.0(3)x \right\} . \quad (2)$$

where  $x$  is the quark light-cone momentum fraction carried in the pion. The transverse renormalisation scale should be 0.5 GeV if the first moment of  $V_\pi$  is to agree with experiment. As a further application of the light-cone wavefunctions, we also compute the probability for a valence quark of momentum fraction  $x$  to have its helicity correlated with that of the anti-quark in the pion. We find a surprisingly large probability  $\sim 45$  % for the quark and anti-quark helicities to be aligned, even though the pion is spin 0. These represent our main results.

Attempts to solve transverse lattice QCD have been renewed in recent years for both the pure gauge theory [4, 5, 6] and mesons [7, 8, 9]. The most successful approaches have employed the original idea [2] of a  $1/N_c$  and colour-dielectric expansion in dynamical fields to approximate the light-cone QCD Hamiltonian on a coarse transverse lattice. For pure gauge theory, to lowest non-trivial order of the expansion, requirements of vacuum stability, Lorentz and gauge invariance alone were found to constrain the coarse lattice Hamiltonian sufficiently accurately for first-principles predictions of the glueball states [5]. Extension of this work to light mesons introduced quarks and imposed a (Tamm-Dancoff) restriction on the number of link fields in Fock space [7]. In previous calculations [8, 9], no more than one link field was allowed in a meson. This effectively restricts the transverse size to  $< 2/3$  fm, which is unrealistic for light mesons. In this case, the correct Hamiltonian could not be accurately identified using Lorentz and gauge invariance alone. Some phenomenology was also needed.

In this paper, we again use the lowest non-trivial order of the colour-dielectric expansion of the hamiltonian, but relax the Tamm-Dancoff cut-off on the space of states. This allows

light mesons to expand to their physical transverse size. It also means that one begins to take account of the full pure-gluon dynamics in the meson sector. While the results are now realistic, we find that it is still necessary to use some phenomenological fitting of masses and decay constants, in addition to optimizing Lorentz covariance, to obtain unambiguous couplings in the coarse-lattice Hamiltonian. We believe this is due to the absence, in the currently employed transverse lattice Hamiltonian, of operators needed to optimize chiral symmetry. We show that such operators would occur at higher order of the colour-dielectric expansion. In the next section, we review and extend the previous work. Section III describes the procedure we employ for fixing the various couplings that appear in the Hamiltonian. Finally, our results for pion observables are discussed in Section IV. Chiral symmetry issues are discussed in an Appendix.

## II. TRANSVERSE LATTICE MESONS

### A. Hamiltonian

We introduce continuum light-cone co-ordinates  $x^\pm = (x^0 \pm x^3)/\sqrt{2}$  and discretize the transverse coordinates  $\mathbf{x} = (x^1, x^2)$  on a square lattice of spacing  $a$ . Lorentz indices  $\mu, \nu$  are split into light-cone indices  $\alpha, \beta \in \{+, -\}$  and transverse indices  $r, s \in \{1, 2\}$ . Subsequent analysis is done to leading order of the  $1/N_c$  expansion of the gauge group  $SU(N_c)$ . Quark fields  $\Psi(x^+, x^-, \mathbf{x})$  in the fundamental representation and gauge potentials  $A_\alpha(x^+, x^-, \mathbf{x})$  in the adjoint representation of  $SU(N_c)$  are associated to the sites of the transverse lattice. Link fields  $M_r(x^+, x^-, \mathbf{x})$ , which we choose to be complex  $N_c \times N_c$  matrices, are associated with the directed link from  $\mathbf{x}$  to  $\mathbf{x} + a\hat{\mathbf{r}}$ . They carry flux from site to site. This use of disordered link variables implies that a coarse transverse lattice is being considered.

For finite spacing  $a$ , the Lagrangian can contain any operators that are local, invariant under transverse lattice gauge symmetries and under Poincaré symmetries manifestly preserved by the lattice cut-off, and renormalisable by dimensional counting with respect to the continuum co-ordinates  $x^\alpha$ . The objective is to obtain an approximation to the light-cone Hamiltonian operator  $P^-$ , that may be diagonalised in a Fock state basis of the above fields. This may be achieved by first fixing to the light-cone gauge  $A_- = 0$ , eliminating non-dynamical fields, then expanding the resulting Hamiltonian in powers of the remaining dynamical fields. Truncation of such a ‘colour-dielectric’ expansion is a valid approximation provided wavefunctions of interest (typically those of the lightest eigenstates) are dominated by few-body Fock states. This is achieved by working in a region of coupling space with sufficiently heavy dynamical fields. This in turn will be found to constrain the transverse lattice spacing  $a$  to be coarse when symmetries and phenomenology are optimized.

The Lagrangian density we consider contains terms up to order  $M^4$  and  $\bar{\Psi}M\Psi$  for the large- $N_c$  theory,

$$\begin{aligned}
L = & \sum_{\mathbf{x}} \int dx^- \sum_{\alpha, \beta = +, -} \sum_{r=1,2} -\frac{1}{2G^2} \text{Tr} \{ F^{\alpha\beta}(\mathbf{x}) F_{\alpha\beta}(\mathbf{x}) \} \\
& + \text{Tr} \{ \bar{D}_\alpha M_r(\mathbf{x}) (\bar{D}^\alpha M_r(\mathbf{x}))^\dagger \} \\
& - \mu_b^2 \text{Tr} \{ M_r M_r^\dagger \} + i \bar{\Psi} \gamma^\alpha (\partial_\alpha + i A_\alpha) \Psi - \mu_f \bar{\Psi} \Psi
\end{aligned}$$

$$\begin{aligned}
& +i\kappa_a \left( \overline{\Psi}(\mathbf{x})\gamma^r M_r(\mathbf{x})\Psi(\mathbf{x}+a\hat{\mathbf{r}}) - \overline{\Psi}(\mathbf{x})\gamma^r M_r^\dagger(\mathbf{x}-a\hat{\mathbf{r}})\Psi(\mathbf{x}-a\hat{\mathbf{r}}) \right) \\
& +\kappa_s \left( \overline{\Psi}(\mathbf{x})M_r(\mathbf{x})\Psi(\mathbf{x}+a\hat{\mathbf{r}}) + \overline{\Psi}(\mathbf{x})M_r^\dagger(\mathbf{x}-a\hat{\mathbf{r}})\Psi(\mathbf{x}-a\hat{\mathbf{r}}) \right) - V_{\mathbf{x}} ,
\end{aligned} \tag{3}$$

where  $F^{\alpha\beta}(\mathbf{x})$  is the continuum field strength in the  $(x^0, x^3)$  planes at each  $\mathbf{x}$ ,

$$\overline{D}_\alpha M_r(\mathbf{x}) = (\partial_\alpha + iA_\alpha(\mathbf{x}))M_r(\mathbf{x}) - iM_r(\mathbf{x})A_\alpha(\mathbf{x}+a\hat{\mathbf{r}}) \tag{4}$$

and the link-field potential is

$$\begin{aligned}
V_{\mathbf{x}} = & -\frac{\beta}{N_c a^2} \sum_{r \neq s} \text{Tr} \left\{ M_r(\mathbf{x}) M_s(\mathbf{x}+a\hat{\mathbf{r}}) M_r^\dagger(\mathbf{x}+a\hat{\mathbf{s}}) M_s^\dagger(\mathbf{x}) \right\} \\
& + \frac{\lambda_1}{a^2 N_c} \sum_r \text{Tr} \left\{ M_r M_r^\dagger M_r M_r^\dagger \right\} + \frac{\lambda_2}{a^2 N_c} \sum_r \text{Tr} \left\{ M_r(\mathbf{x}) M_r(\mathbf{x}+a\hat{\mathbf{r}}) M_r^\dagger(\mathbf{x}+a\hat{\mathbf{r}}) M_r^\dagger(\mathbf{x}) \right\} \\
& + \frac{\lambda_4}{a^2 N_c} \sum_{\sigma=\pm 2, \sigma'=\pm 1} \text{Tr} \left\{ M_\sigma^\dagger M_\sigma M_{\sigma'}^\dagger M_{\sigma'} \right\} .
\end{aligned} \tag{5}$$

We have defined  $M_r = M_{-r}^\dagger$  and hold  $\overline{G} \rightarrow G\sqrt{N_c}$  finite as  $N_c \rightarrow \infty$ . To this action we could in principle add allowed operators at order  $M^6$ ,  $(\overline{\Psi}\Psi)^2$ ,  $\Psi M^2 \Psi$ , and so on. It should therefore be understood as the truncation of an expansion in powers of the fields. Strictly speaking, this expansion should be performed for the light-cone gauge-fixed Hamiltonian in terms of dynamical fields only.

In the chiral representation,  $\Psi^\dagger = (u_+^*, v_+^*, v_-^*, u_-^*)/2^{1/4}$  decomposes into complex fermion fields  $v$  ( $u$ ) with a helicity subscript  $h = \pm$  denoting the sign of the eigenvalue of  $\gamma^5$ . In light-cone gauge  $A_- = 0$ ,  $A_+$  and  $v_\pm$  are non-dynamical (independent of light-cone time  $x^+$ ) and are eliminated at the classical level using the equations of motion

$$(\partial_-)^2 A_+ = \frac{G^2}{2} \left( J^+ - \frac{1}{N} \text{Tr} J^+ \right) \tag{6}$$

$$i\partial_- v_h = \frac{\mu_f}{\sqrt{2}} F_{-h} , \tag{7}$$

where we have defined

$$\begin{aligned}
F_h(\mathbf{x}) = & -u_h(\mathbf{x}) + \frac{\kappa_s}{\mu_f} \sum_r \left( M_r(\mathbf{x}) u_h(\mathbf{x}+a\hat{\mathbf{r}}) + M_r^\dagger(\mathbf{x}-a\hat{\mathbf{r}}) u_h(\mathbf{x}-a\hat{\mathbf{r}}) \right) \\
& + \frac{h i \kappa_a}{\mu_f} \left\{ M_1(\mathbf{x}) u_{-h}(\mathbf{x}+a\hat{\mathbf{1}}) - h i M_2(\mathbf{x}) u_{-h}(\mathbf{x}+a\hat{\mathbf{2}}) \right. \\
& \left. - M_1^\dagger(\mathbf{x}-a\hat{\mathbf{1}}) u_{-h}(\mathbf{x}-a\hat{\mathbf{1}}) + h i M_2^\dagger(\mathbf{x}-a\hat{\mathbf{2}}) u_{-h}(\mathbf{x}-a\hat{\mathbf{2}}) \right\} ,
\end{aligned} \tag{8}$$

$$\begin{aligned}
J^+(\mathbf{x}) = & i \sum_r \left( M_r(\mathbf{x}) \overset{\leftrightarrow}{\partial}_- M_r^\dagger(\mathbf{x}) + M_r^\dagger(\mathbf{x}-a\hat{\mathbf{r}}) \overset{\leftrightarrow}{\partial}_- M_r(\mathbf{x}-a\hat{\mathbf{r}}) \right) \\
& + \sum_h u_h(\mathbf{x}) u_h^\dagger(\mathbf{x}) ,
\end{aligned} \tag{9}$$

The lightcone Hamiltonian, expressed in terms of the remaining dynamical fields  $u_\pm(\mathbf{x})$  and  $M_r(\mathbf{x})$ , may be obtained from the action (3) in the standard way [3]

$$\begin{aligned}
P^- = & \int dx^- \sum_{\mathbf{x}} \frac{G^2}{4} \left( \text{Tr} \left\{ J^+ \frac{1}{(i\partial_-)^2} J^+ \right\} - \frac{1}{N_c} \text{Tr} \{ J^+ \} \frac{1}{(i\partial_-)^2} \text{Tr} \{ J^+ \} \right) \\
& + \frac{\mu_f^2}{2} \sum_h \left( F_h^\dagger \frac{1}{i\partial_-} F_h \right) + V_{\mathbf{x}}[M] .
\end{aligned} \tag{10}$$

Under certain reasonable assumptions [8], the Hamiltonian (10) is a truncation of the most general Hamiltonian to order  $M^4$  and  $uMu$ . It also contains some, but not all, allowed operators at order  $uM^2u$  and  $u^4$ . In particular, it contains the combination  $J^+\partial_-^2J^+$ , which is responsible for confinement in the lattice theory of states singlet under residual  $x^-$ -independent gauge transformation [2]. The various parameters  $G, \mu_f, \kappa_a, \kappa_s, \mu_b, \lambda_1, \lambda_2, \lambda_4, \beta$ , as well as ones that would appear at higher orders of the colour-dielectric expansion, are coupling constants that will run with the cut-off(s) in the theory. In principle, this running could be determined by performing renormalisation group transformations from QCD at short distance scales. However, on a coarse lattice, weak-coupling perturbation theory is not available, and such an approach become unworkable. One may also treat the problem as an effective field theory, fixing couplings phenomenologically. Even in this case, one may constrain the parameters from first principles by empirically tuning them to minimize the violation of continuum symmetries. In the case of pure gauge theories, at lowest order of the colour-dielectric expansion, this gave a quite accurate estimate of the running couplings, without the need to resort to ‘phenomenology’ [5]. For meson calculations with our choice of Hamiltonian (10), additional phenomenological constraints must be used to obtain unambiguous values for the coupling constants, although symmetry requirements do strongly constrain them.

Of the other generators of the Poincaré algebra,  $P^\nu, M^{\mu\nu}$ , the following can be derived canonically at  $x^+ = 0$

$$P^+ = \int dx^- \sum_{\mathbf{x}, s, h} 2 \text{Tr} \{ \partial_- M_s(\mathbf{x}) \partial_- M_s(\mathbf{x})^\dagger \} + i u_h^* \partial_- u_h , \quad (11)$$

$$M^{-+} = \int dx^- \sum_{\mathbf{x}, s, h} x^- \left\{ 2 \text{Tr} \{ \partial_- M_s(\mathbf{x}) \partial_- M_s(\mathbf{x})^\dagger \} + \frac{i}{2} u_h^* \overleftrightarrow{\partial}_- u_h \right\} , \quad (12)$$

$$M^{+r} = - \int dx^- \sum_{\mathbf{x}, s, h} 2 \left( x^r + \frac{a}{2} \delta^{rs} \right) \text{Tr} \{ \partial_- M_s(\mathbf{x}) \partial_- M_s(\mathbf{x})^\dagger \} + i x^r u_h^* \partial_- u_h . \quad (13)$$

Note that these are all kinematic operators, quadratic in fields.  $P^+$  and  $M^{-+}$  generate translations and boosts respectively in the  $x^-$  direction and are unaffected by the transverse lattice cut-off. The cut-off effects on the boost-rotation operator  $M^{+r}$  are discussed further in the next section.

## B. Space of states

For the construction of a Fock space of the dynamical fields  $M_r$  and  $u_h$ , it is convenient to Fourier transform the fields in the  $x^-$  co-ordinate only. Thus, we introduce a Fock space operator  $a_{r,ij}^\dagger(k^+, \mathbf{x})$  which creates a ‘link-parton’ with light-cone momentum  $k^+$ , carrying colour  $i \in \{1, \dots, N_c\}$  at site  $\mathbf{x}$  to colour  $j$  at site  $\mathbf{x} + a\hat{\mathbf{r}}$ ;  $a_{-r,ij}^\dagger$  creates an oppositely oriented link-parton. Likewise,  $b_{h,i}^*(k^+, \mathbf{x})$  creates a ‘quark-parton’ of helicity  $h$ , colour  $i$ , momentum  $k^+$  at site  $\mathbf{x}$ , while  $d^*$  does the same for anti-quarks. We have

$$[a_{\lambda,ij}(k^+, \mathbf{x}), a_{\rho,kl}^*(\tilde{k}^+, \mathbf{y})] = \delta_{ik} \delta_{jl} \delta_{\lambda\rho} \delta_{\mathbf{xy}} \delta(k^+ - \tilde{k}^+) , \quad (14)$$

$$[a_{\lambda,ij}(k^+, \mathbf{x}), a_{\rho,kl}(\tilde{k}^+, \mathbf{y})] = 0 , \quad (15)$$

$$\{b_{h,i}(k^+, \mathbf{x}), b_{h',j}^*(\tilde{k}^+, \mathbf{y})\} = \delta_{ij} \delta_{hh'} \delta_{\mathbf{xy}} \delta(k^+ - \tilde{k}^+) , \quad (16)$$

$$\{b_{h,i}(k^+, \mathbf{x}), b_{h',j}(\tilde{k}^+, \mathbf{y})\} = 0 , \quad (17)$$

where  $\lambda$  and  $\rho \in \{\pm 1, \pm 2\}$  denote the orientations of link variables in the  $(x^1, x^2)$  plane,  $a_{\lambda,ij}^* = a_{\lambda,ji}^\dagger$ , and similar anti-commutators exist for  $d$ . Fock space is already diagonal in the light-cone momentum  $P^+$  and serves as a basis for finding the eigenfunctions  $P^-$ , the light-cone wavefunctions. As usual in light-cone quantisation (without zero modes), the Fock vacuum state  $|0\rangle$  is an exact eigenstate of  $P^-$ .

Further cut-offs, apart from the transverse lattice, must be applied to Fock space to make it finite-dimensional. We will use DLCQ [10, 11] to discretize light-cone momentum, which amounts to compactifying  $x^-$  on circle of circumference  $\mathcal{L} = 2\pi K/P^+$ , where  $K$  is a positive integer, with periodic (anti-periodic) boundary conditions for  $M(u)$ . Eventually, we will extrapolate observables to  $K = \infty$ . The use of anti-periodic boundary conditions is desirable because it tends to improve convergence as  $K \rightarrow \infty$ . However, one cannot consistently have anti-periodic boundary conditions for both bosons and fermions in a theory with Yukawa-type interactions.

To reduce the size of Fock space still further, it will be convenient to impose a separate Tamm-Dancoff cut-off on the maximum number of partons in Fock space, studying the theory as this cutoff is raised. Since the large  $N_c$  limit automatically restricts to a quark-antiquark pair in the meson sector, this effectively means a cut-off on the number of link-partons. A general meson state of light-cone momentum  $P^+$ , which is translationally invariant in the transverse direction, takes the form

$$\begin{aligned} |\psi(P^+)\rangle = & \frac{2a\sqrt{\pi}}{\sqrt{N_c}} \sum_{\mathbf{x}} \sum_{h,h'} \int_0^{P^+} dk_1^+ dk_2^+ \delta(P^+ - k_1^+ - k_2^+) \left\{ \psi_{hh'}(x_1, x_2) b_h^\dagger(k_1^+, \mathbf{x}) d_{h'}^\dagger(k_2^+, \mathbf{x}) |0\rangle \right\} \\ & + \frac{2a\sqrt{\pi}}{N_c} \sum_{\mathbf{x}} \sum_{h,h',r} \int_0^{P^+} \frac{dk_1^+ dk_2^+ dk_3^+}{P^+} \delta(P^+ - k_1^+ - k_2^+ - k_3^+) \\ & \times \left\{ \psi_{h(r)h'}(x_1, x_2, x_3) b_h^\dagger(k_1^+, \mathbf{x}) a_r^\dagger(k_2^+, \mathbf{x}) d_{h'}^*(k_3^+, \mathbf{x} + a\hat{\mathbf{r}}) |0\rangle \right. \\ & \left. + \psi_{h(-r)h'}(x_1, x_2, x_3) b_h^\dagger(k_1^+, \mathbf{x} + a\hat{\mathbf{r}}) a_{-r}^\dagger(k_2^+, \mathbf{x}) d_{h'}^*(k_3^+, \mathbf{x}) |0\rangle \right\} \\ & + \frac{2a\sqrt{\pi}}{\sqrt{N_c^3}} \sum_{\mathbf{x}} \sum_{h,h',r,s} \int_0^{P^+} \frac{dk_1^+ dk_2^+ dk_3^+ dk_4^+}{(P^+)^2} \delta(P^+ - k_1^+ - k_2^+ - k_3^+ - k_4^+) \\ & \times \left\{ \psi_{h(rs)h'}(x_1, x_2, x_3, x_4) b_h^\dagger(k_1^+, \mathbf{x}) a_r^\dagger(k_2^+, \mathbf{x}) a_s^\dagger(k_3^+, \mathbf{x} + a\hat{\mathbf{r}}) d_{h'}^*(k_4^+, \mathbf{x} + a\hat{\mathbf{r}} + a\hat{\mathbf{s}}) |0\rangle \right. \\ & + \psi_{h(r-s)h'}(x_1, x_2, x_3, x_4) b_h^\dagger(k_1^+, \mathbf{x}) a_r^\dagger(k_2^+, \mathbf{x}) a_{-s}^\dagger(k_3^+, \mathbf{x} + a\hat{\mathbf{r}} - a\hat{\mathbf{s}}) d_{h'}^*(k_4^+, \mathbf{x} + a\hat{\mathbf{r}} - a\hat{\mathbf{s}}) |0\rangle \\ & + \psi_{h(-rs)h'}(x_1, x_2, x_3, x_4) b_h^\dagger(k_1^+, \mathbf{x} + a\hat{\mathbf{r}}) a_{-r}^\dagger(k_2^+, \mathbf{x}) a_s^\dagger(k_3^+, \mathbf{x}) d_{h'}^*(k_4^+, \mathbf{x} + a\hat{\mathbf{s}}) |0\rangle \\ & \left. + \psi_{h(-r-s)h'}(x_1, x_2, x_3, x_4) b_h^\dagger(k_1^+, \mathbf{x} + a\hat{\mathbf{r}}) a_{-r}^\dagger(k_2^+, \mathbf{x}) a_{-s}^\dagger(k_3^+, \mathbf{x} - a\hat{\mathbf{s}}) d_{h'}^*(k_4^+, \mathbf{x} - a\hat{\mathbf{s}}) |0\rangle \right\} + \dots , \end{aligned} \quad (18)$$

where states with up to two links have been explicitly displayed. In (18),  $\dagger$  acts on gauge indices and  $x_1 = k_1^+/P^+$  etc., are light-cone momentum fractions. Only gauge singlet combinations under residual gauge transformations in  $A_- = 0$  gauge can contribute to states of finite energy [2]. Because pair production of quarks and mixing with glueballs is suppressed at large  $N_c$ , the states (18) provide a description of the valence quark content

of flavour non-singlet mesons. Thus one should implicitly understand a distinct flavour label on the quark and anti-quark, which is redundant. For states that are translationally invariant in the transverse direction, the transverse co-ordinate argument in wavefunctions may be suppressed. The sequence of orientations  $\lambda, \rho, \dots$  of link variables, together with the  $P^+$  momentum fractions  $x_1, x_2, \dots$  and quark helicities  $h, h'$  are sufficient to encode the structure of Fock states contributing to the boundstate. Thus, a general Fock state may be labelled

$$|(x_1, h), (x_2, \lambda), \dots, (x_{n-1}, \rho), (x_n, h')\rangle . \quad (19)$$

The expansion (18) may be represented by a planar (large- $N_c$ ) diagram notation shown in Fig. 1. This will be helpful when enumerating the matrix elements of the Hamiltonian.

The transverse momentum operator is not directly defined because of the lattice regulator, but one may introduce transverse momentum  $\mathbf{P}$  by application of the boost-rotation operator  $M^{+r}$ . Let  $|(x_1, \mathbf{x}_1), \dots, (x_n, \mathbf{x}_n)\rangle$  denote an  $n$ -parton Fock state.  $\mathbf{x}_p$  is the transverse position and  $x_p$  the  $P^+$  momentum fraction of the  $p^{\text{th}}$  parton (conventionally we take transverse position to be the midpoint of a link, for link fields). Using (13) we find

$$\exp \left[ -iM^{+r} P_r / P^+ \right] |(x_1, \mathbf{x}_1), \dots, (x_n, \mathbf{x}_n)\rangle = \exp \left[ i\mathbf{P} \cdot \sum_{p=1}^n x_p \mathbf{x}_p \right] |(x_1, \mathbf{x}_1), \dots, (x_n, \mathbf{x}_n)\rangle . \quad (20)$$

Therefore, the net effect is to add phase factors into matrix elements of  $P^-$  between Fock states at  $\mathbf{P} = 0$ . In a Poincaré covariant or a free theory, the transformation (20) applied to eigenstates of  $P^-$  (18) would be sufficient to generate eigenstates of  $P^-$  at non-zero  $\mathbf{P}$ . However, the lattice regulator spoils Poincaré covariance and in general one must re-diagonalise  $P^-$  after boosting Fock states by (20). Thus the eigenfunctions  $\psi$  in (18) for  $P^-$  will become functions of  $\mathbf{P}$  also.

The state is normalised covariantly

$$\langle \psi(P_1^+, \mathbf{P}_1) | \psi(P_2^+, \mathbf{P}_2) \rangle = 2P_1^+ (2\pi)^3 \delta(P_1^+ - P_2^+) \delta(\mathbf{P}_1 - \mathbf{P}_2) \quad (21)$$

if

$$\begin{aligned} 1 = & \int_0^1 dx \sum_{h,h'} |\psi_{hh'}(x, 1-x)|^2 + \int_0^1 dx_1 dx_2 \sum_{h,\lambda,h'} |\psi_{h(\lambda)h'}(x_1, x_2, 1-x_1-x_2)|^2 \\ & + \int_0^1 dx_1 dx_2 dx_3 \sum_{h,\lambda,\rho,h'} |\psi_{h(\lambda\rho)h'}(x_1, x_2, x_3, 1-x_1-x_2-x_3)|^2 + \dots . \end{aligned} \quad (22)$$

for any  $\mathbf{P}_1, \mathbf{P}_2$ . This also ensures that the light-cone momentum sum rule is satisfied, even at finite DLCQ cutoff  $K$ , since translation invariance in the  $x^-$  direction is preserved by DLCQ.

Since there is  $90^\circ$  rotational symmetry about  $x^3$  for a state with  $\mathbf{P} = 0$ , it is possible to distinguish the angular momentum projections  $\mathcal{J}_3 \bmod 4$ . There is also exact symmetry under  $\mathcal{G}$ -parity, charge conjugation  $\mathcal{C}$ , and transverse reflections in the  $x^1$  and  $x^2$  direction,  $\mathcal{P}_1, \mathcal{P}_2$ . Although the parity  $\mathcal{P} = \mathcal{P}_1 \mathcal{P}_2 \mathcal{P}_3$  is dynamical and in general broken, one can associate a parity to boundstates from their behaviour under the free particle limit of  $\mathcal{P}_3$ . Indeed, there is a  $Z_2$  kinematic symmetry

$$\mathcal{P}_f \psi_{hh'}(1-x, x) \rightarrow \psi_{hh'}(x, 1-x) , \quad (23)$$

which corresponds to the free  $\mathcal{P}_3$  operation in the zero-link sector, that is exact at any cut-off  $K$ . In this way, one has enough information to identify the  $\mathcal{J}^{PC}$  structure of light states unambiguously.

In general, we will find that the  $0^{-+}$  pion mass is split from the  $1^{--}$  rho mass. Due to violations of covariance, the  $\mathcal{J}_3 = 0$  component of the rho ( $\rho_0$ ) will also split from its  $\mathcal{J}_3 = \pm 1$  components ( $\rho_{\pm}$ ) which are always degenerate on the transverse lattice at  $\mathbf{P} = 0$ . In view of the low-energy nature of the truncation of the colour-dielectric expansion, we do not analyse heavier mesons, although their eigenfunctions are obtained as a by product of our calculations.

### C. Renormalisation

We have constructed a gauge theory with transverse lattice and Tamm-Dancoff cut-offs that we do not intend to extrapolate and a DLCQ cut-off that we do. The first step in the renormalisation process is to ensure finiteness of physical observables in the limit  $K \rightarrow \infty$ . It turns out that divergences exist but they require only infinite and finite self-energy counterterms that renormalise existing parton mass terms in the light-cone Hamiltonian. The remaining cut-offs that are not extrapolated obviously violate Lorentz covariance. This violation can however be minimized by appropriate finite renormalisation all of the couplings appearing in  $P^-$  (10). In this section we describe our procedure for performing these finite and infinite renormalisations.

It is convenient to use one of the parameters of the Hamiltonian to set the dimensionful scale of the theory and define dimensionless versions of the others. Conventionally we will use  $\bar{G}$  to set the scale, which has the dimensions of mass. It will later be related to the QCD mass scale by calculation of the heavy source potential [6]. The following dimensionless parameters are then introduced:

$$\begin{aligned} \frac{\mu_b}{\bar{G}} \rightarrow m_b \quad ; \quad \frac{\mu_f}{\bar{G}} \rightarrow m_f \quad ; \quad \frac{\kappa_a \sqrt{N_c}}{\bar{G}} \rightarrow k_a \quad ; \quad \frac{\kappa_s \sqrt{N_c}}{\bar{G}} \rightarrow k_s \quad ; \\ \frac{\lambda_i}{\bar{G}^2} \rightarrow l_i \quad (i = 1, 2, 4) \quad ; \quad \frac{\beta}{\bar{G}^2} \rightarrow b \quad . \end{aligned} \quad (24)$$

Since we will need to study the meson eigenfunctions of  $P^-$  as a function of  $P^+$  and  $\mathbf{P}$ , let us write, for these eigenfunctions,

$$2P^+P^- = \mathcal{M}^2 + R(\mathbf{P}) \quad . \quad (25)$$

such that  $R(0) = 0$ .  $\mathcal{M}^2$  is the invariant mass (squared). We begin with  $\mathbf{P} = 0$ , in which case the non-zero Fock space matrix elements of the dimensionless invariant mass operator

$$\langle (y_1, h_1), (y_2, \sigma), \dots, (y_{n-1}, \tau), (y_n, h_2) | 2P^+P^- / \bar{G}^2 | (x_1, h'_1), (x_2, \lambda), \dots, (x_{n-1}, \rho), (x_n, h'_2) \rangle \quad (26)$$

are enumerated in figs. 2(i)-(xiii) and table I. A number of comments are necessary to explain these amplitudes. We have defined

$$\text{Rot}[\lambda, \rho] \equiv \epsilon_{|\lambda||\rho|} \text{Sgn}[\lambda] \text{Sgn}[\rho] \quad . \quad (27)$$



In the planar diagram vertices of Fig. 2, light-cone momentum fraction  $(x, y, z)$ , quark helicity  $(h, h')$ , and link-field orientation  $(\lambda, \rho, \sigma, \tau)$  labels are given where necessary. Lines with a bar denote the  $x^+$ -instantaneous propagators  $\partial_-^{-1}$  and  $\partial_-^{-2}$  for  $v$  quarks and  $A_+$  gauge fields respectively. ‘P’ denotes that a principal value prescription is used when integrating light-cone continuum momentum fraction across singularities. For simplicity, we have not shown vertices involving only anti-quarks, which are similar to those involving only quarks. To these diagrams we add planar spectator lines which go to make up the full gauge singlet Fock state.

At finite transverse lattice spacing  $a$ , but before the light-cone DLCQ cutoff  $K$  is imposed, the theory is behaving like a continuum  $1 + 1$ -dimensional gauge theory coupled to a set of fundamental fermion and adjoint scalar fields [12]. Although super-renormalisable in the  $1 + 1$ -dimensional sense, the light-cone quantisation in light-cone gauge introduces its own characteristic divergences due to the presence of non-local instantaneous interactions. Those originating from the instantaneous gluon propagator  $1/\partial_-^2$  are dealt with by the principal value prescription in the manner established by ‘t Hooft [13]. Those originating from the instantaneous quark propagator  $1/\partial_-$  have been studied by Burkardt [14], whose analysis we briefly recall.

A basic one-loop logarithmic divergence occurs in the quark self-energy as represented in the Light-cone Perturbation Theory diagram of Fig. 3(i) as the quark loop momentum vanishes. The cubic vertices are of the same type, with coupling either  $m_f k_a$  or  $m_f k_s$ , once the orientations of the intermediate link fields have been summed over. The divergences are cancelled, in these diagrams and any others obtained by adding spectators, by an infinite quark ‘kinetic’ mass counterterm in the Hamiltonian (Fig. 3(ii))

$$\frac{(k_a^2 + k_s^2)}{\pi} \int_0^x \frac{dy}{y} . \quad (28)$$

This is not sufficient for the divergences in the two-loop diagrams of Fig. 4(i)(ii)(iii) to cancel. One may add a finite kinetic mass counterterm  $\delta m^2$ , adjusted at order  $(k_a^2, k_s^2)$ , to produce finite results when Fig. 4(iv) is included. Higher-loop generalisations of the same diagrams are also rendered finite by adjusting  $\delta m^2$  at higher orders in  $k_a$  and  $k_s$ . Dressing loop diagrams with instantaneous gluon lines (e. g. Fig. 5) renders them individually finite. As in Ref. [14], our own checks of these statements for the transverse lattice theory have been done only in perturbation theory, but we will assume they are true to all orders. It was also shown in Ref. [14], by means of simple cases, that choosing the correct counterterm  $\delta m^2$  was equivalent to restoring parity invariance, which is not manifest in light-cone co-ordinates.

By adjusting the finite counterterm  $\delta m^2$ , one ensures that the  $K \rightarrow \infty$  limit can be taken when DLCQ is used. However, it was pointed out by Burkardt that, while this ensures a finite answer for the  $K \rightarrow \infty$  limit of the self-energy, the use of a momentum-independent mass counterterm in DLCQ will not yield the same as the covariant answer for the same couplings. In effect DLCQ produces a finite violation of covariance. This is one of a number of sources covariance violation in our calculation. Rather than analysing how one might minimize the individual violations — it is not obvious which are the most significant — we will perform overall covariance tests on the boundstate wavefunctions that are the end-product.

A Tamm-Dancoff cut-off on the maximum number of link fields in a state also violates covariance. In principle, this can be compensated by introducing spectator-dependent coun-

terterms [15]. In practice, that will lead to too many couplings for viable calculation at a physically reasonable choice of Tamm-Dancoff cut-off. However, it is necessary for finiteness of the quark self-energy to use spectator-dependent finite counterterms  $\delta m^2$ . Therefore, we must introduce separate counterterms  $\delta m_p^2$  for the Fock sector containing  $p$  links (note that the sector with  $p$  maximum has no finite or infinite quark self-energy counterterms). These are adjusted to produce finite quark self energy in addition to optimization of covariance of hadron wavefunctions. Since we work at the level of hadrons, the quark self-energy is tested indirectly. A tachyonic quark self-energy, whether divergent or not, would be signalled by tachyonic behaviour in the lightest hadron mass. Therefore, we test for absence of such a divergence in the pion mass as  $K \rightarrow \infty$ . A positive divergent quark self-energy would artificially suppress the lowest Fock sectors, that are subject to loop corrections and counterterms, in the hadron wavefunction as  $K \rightarrow \infty$  (the hadron mass may remain finite). Therefore, we test for absence of this suppression, in particular by fitting  $f_\pi$  which is a measure of the  $p = 0$  Fock component.

In summary, taking the  $K \rightarrow \infty$  limit with a Tamm-Dancoff cut-off on link fields in place, one must introduce infinite and spectator-dependent finite self-energy counterterms. Even though the theory is now finite, Poincare covariance is still violated by the finite transverse lattice spacing  $a$ , the Tamm-Dancoff cutoff, and by the use of momentum-independent finite-mass counterterms  $\delta m_p^2$ . We propose to minimize these violations by finitely renormalising all the couplings available in  $P^-$ .

For perfectly relativistic dispersion,  $R(\mathbf{P}) = |\mathbf{P}|^2$  for every eigenfunction in eq. (25); this will receive corrections on the coarse transverse lattice. To quantify the covariance violation we will expand the dispersion relation for each boundstate

$$R(\mathbf{P}) = c^2|\mathbf{P}|^2 + O(\mathbf{P}^4) . \quad (29)$$

The transverse speed of light  $c$  will in general differ from one (the speed in the  $x^3$  direction). A simple criterion, which worked well in previous studies, is to minimize this difference in the low lying eigenstates of  $P^-$ , ignoring the anharmonic terms in  $R$ .

The same procedure may be carried out for glueball boundstates to constrain the pure-gluon interactions in the Hamiltonian, independently of the meson sector (at large  $N_c$ ). In addition, the rotational invariance of the potential between heavy sources may be optimized. These latter tests have been described in detail in previous work [5]. We will use the string tension  $\sqrt{\sigma}$  from the potential to set the QCD scale from experiment.

The transverse lattice lagrangian (3) contains terms that also violate chiral symmetry explicitly, via the couplings  $m_f$  and  $k_s$ . Since we work at the level of hadrons, a measure of chiral current non-conservation is provided by the pion mass in a covariant stable theory, as a result of the PCAC theorem. This measure loses accuracy if the theory also has significant explicit covariance violation, as in our case. The explicit violation of chiral symmetry could be minimized by tuning further chiral-symmetry violating counterterms, which we discuss in the appendix. However, these lie at higher order of the colour-dielectric expansion. In the present calculation, we finitely renormalize the hamiltonian to fit the experimental pion mass, since this is naively a measure of chiral current conservation. Since the explicit violation of chiral symmetry is actually larger than that suggested by  $\mathcal{M}_\pi$ , we find that we must also fit the experimental rho mass in order to maintain a realistic pi-rho splitting.

Thus, in addition to optimizing covariance via boundstate dispersion, we are proposing to fit four experimental numbers  $\mathcal{M}_\pi$ ,  $\mathcal{M}_\rho$ ,  $f_\pi$ , and  $\sqrt{\sigma}$  in order to accurately determine

the couplings in our effective hamiltonian  $P^-$ . Since QCD with degenerate flavours contains only two fundamental parameters, the transverse lattice hamiltonian is not determined from first principles. However, as described above, direct tests of parity and chiral symmetry might allow one to reduce the number of phenomenological parameters further. We leave this for future work.

### III. DETERMINATION OF HAMILTONIAN PARAMETERS

In order to reduce the number of coupling variables in the minimization process, this is done in two stages. First, we examine glueball eigenfunctions of  $P^-$ , that contain only link-fields, and the rotational invariance of the groundstate potential between two heavy sources of colour. Here we follow, with one exception, exactly the same procedure used in refs. [5] and so omit all details. The exception is that, instead of using anti-periodic boundary conditions for link fields in  $x^-$ , we re-did the calculations with periodic boundary conditions in order to be consistent with the conditions used in the meson sector later. Note that these ‘pure-glue’ calculations extrapolate both  $K$  and the Tamm-Dancoff cut-off, constraining very precisely the couplings in  $P^-$  relevant to that sector  $(l_1, l_2, l_3, b, m_b)$  when covariance is optimized. It is not necessary at this stage to use any phenomenological input.

We searched for a trajectory in coupling space that optimized the Poincaré covariance of glueball wavefunctions and the potential between heavy sources of colour. A fairly well-defined one-parameter trajectory is picked out. We chose the best point on that trajectory, which in effect fixes  $a$ , corresponding to a value of the link field mass  $m_b = 0.276$ . At this point, we find  $\bar{G} \approx 2.75\sqrt{\sigma}$  and  $a\bar{G} \approx 4$ , where  $\sigma$  is the string tension of the asymptotically linear potential found between two heavy sources. If one takes  $\sqrt{\sigma} = 440$  MeV, then  $\bar{G} \approx 1200$  MeV and  $a \approx 2/3$  fm. The values of the other couplings determined by this point are shown in table II.

Having fixed a subset of the couplings, we fix the remaining ones sensitive only to the meson sector. We investigated the Tamm-Dancoff-cutoff up to four links, but show results for a three-link cut-off, since a better sampling of couplings is achievable in this case. The transverse speed of light  $c$  is optimized in the dispersion of the pion and each component of the rho, together with the difference between the calculated mass  $\mathcal{M}_\pi$  and the physical value. As described in the previous section, we find we must include fits to the physical values of  $\mathcal{M}_\rho$  and  $f_\pi$  in the optimization procedure in order to accurately pin down the remaining undetermined couplings of the Hamiltonian, which are shown in table II.

Table III shows information on the pi and rho states at these couplings. One notes that the spin  $\pm 1$  projections of the rho still badly violate covariance, splitting the Lorentz multiplet and having asymmetrical dispersion. Since the rho is not yet behaving covariantly overall, we do not attempt a detailed phenomenological analysis of the resulting wavefunctions. On the other hand, we are able to achieve a relatively symmetrical dispersion for the pion, with intercept  $\mathcal{M}_\pi = 171$  MeV and decay constant  $f_\pi = 132$  MeV, close to the experimental values. (The exact values would be obtainable with a sufficiently fine sweep of couplings).

We checked that no Fock sectors are being artificially suppressed and that the truncation to no more than three links is not causing severe ‘finite-volume’ effects. Table IV shows that the peak in the transverse spatial distribution of the pion wavefunction is well-accomodated by the three-link cut-off (results are similar for the rho). However, the tail of the wavefunc-

tion at four and higher links may contain a significant total probability, which will affect observables sensitive to very small transverse momenta. Therefore, in this paper we restrict our attention to observables integrated over all available transverse momenta. Indeed, when varying the Tamm-Dancoff cut-off above three links, we find very little change in the observables investigated below.

## IV. PION OBSERVABLES

### A. Valence quark structure function

The valence quark distribution function is defined as

$$V(x) = \sum_{h,h'} |\psi_{hh'}(x, 1-x)|^2 + \sum_{\lambda} \sum_{h,h'} \int_0^{1-x} dy |\psi_{h(\lambda)h'}(x, y, 1-x-y)|^2 \\ + \sum_{\lambda,\rho} \sum_{h,h'} \int_0^{1-x} dy \int_0^{1-x-y} dz |\psi_{h(\lambda\rho)h'}(x, y, z, 1-x-y-z)|^2 + \dots \quad (30)$$

It is the probability for a quark to carry light-cone momentum fraction  $x$ . The result we find for  $V(x)$  in the pion on the transverse lattice in the three-link truncation is shown in Fig. 6. The raw (discrete) DLCQ data for  $K = 10, 12, 15, 20$  are displayed together with an extrapolation to  $K \rightarrow \infty$ . To produce this, at each  $K$  data is fit to the form

$$xV(x) = (1-x)^\beta x^\alpha (a + b\sqrt{x} + cx) \quad (31)$$

$xV$  is directly the momentum distribution and is easier to extrapolate since it vanishes at  $x = 0$ . We note that the simple form  $x^\alpha(1-x)^\beta$ , used to parameterize early experimental data, is not sufficient to fit our result. It is necessary to drop the  $x = 1/2K$  and  $x = 1 - 1/2K$  points from this analysis since they do not join smoothly to the rest of the distribution. This is because endpoint data are prone to artifacts resulting from the vanishing of some of the interactions in Table I. The smooth curves at each  $K$  are then extrapolated pointwise, by a (good) fit to a quadratic in  $1/K$ , for a large set of values in the interval  $0.1 < x < 0.9$ . The grey region represents the uncertainty from the extrapolation only.

The extrapolated data fits the form (31) with  $\beta = 0.33(2)$ ,  $\alpha = 0.3(1)$ ,  $a = 0.33(3)$ ,  $b = -1.1(2)$ ,  $c = 2.0(3)$ . The errors are from the extrapolation only. Bearing in mind that the extrapolation is based on fits to data that do not cover the endpoint regions, the true errors on  $\alpha$  and  $\beta$  are likely to be much larger. From the first moment  $\langle xV_\pi \rangle = \int_0^1 xV_\pi(x)dx$ , we find that 32% of meson light-cone momentum is carried by the quarks, with the same carried by the anti-quarks. In the range  $0.1 < x < 0.9$ , over which there is some measure of control, the result for  $V_\pi$  is reminiscent of the constant  $V_\pi = 1$  distribution resulting from the chiral limit of chiral quark models (see Ref. [16] and references therein). However, because of the rapid rise at small  $x$ , which is expected on general grounds from Regge-type behaviour [17], the flat part of the distribution is at  $V \sim 0.7$ . Moreover, in the chiral quark models, all the light-cone momentum is carried by quarks, while here 36% is carried by the link fields representing gluonic degrees of freedom.

A well-defined transverse scale is associated with  $V(x)$  above, namely, the transverse lattice spacing  $a$ . If we were to repeat the calculation at a different  $a$ , one would expect

to see an evolution of  $V$  as a result of the changing wavefunctions. In practice, the current transverse lattice method is only able to explore a small window in  $a$  — small enough to suppress discretization errors but large enough for the use of massive disordered link fields — which is too small to reliably see evolution. Perturbative evolution equations typically use a different renormalisation scheme, so there is no simple matching between scales. This problem is common to most non-perturbative approaches to QCD, except Euclidean lattice QCD where (moments of)  $V$  can be calculated in schemes matched to perturbation theory [18]. In low-energy effective theories for pion structure, such as QCD sum rules [19, 20], chiral quark, colour-dielectric transverse lattice, truncated Dyson-Schwinger [21], etc., one is reduced to fixing the scale for input to perturbative evolution equations heuristically by demanding, say, agreement of the first moment of  $V$  with experiment at some scale.

If we demand that  $\langle xV_\pi \rangle \approx 0.21$  at a scale of 2 GeV, as suggested by the analysis of E615 and NA10 pion-nucleon Drell-Yan data by Sutton et. al. [22] for the valence quark distribution, then the scale associated to our result, if it were used as input for leading order non-singlet evolution, is  $\mu \approx 500\text{MeV}$ ; this is reasonable given that  $a^{-1} = 300\text{MeV}$ . In Fig. 7 we show our result for  $xV_\pi(x)$  evolved to 6.6GeV and compared with the raw data for the valence distribution deduced by E615 [23] by combining data over scales 4 – 8.5 GeV. For completeness, we also show fits to  $xV = x^\alpha(1-x)^\beta$  produced by earlier experiments NA10 [24] and NA3 [25]. In the valence region  $x > 0.5$ , our result agrees with the most recent experiment, which claims a more accurate representation at large  $x$ . At smaller  $x$  there is not much agreement, either between experiments or with our result. This is hardly surprising given the sensitivity of this region to assumptions about the sea quarks or their measurement. In fact, our calculation contains no sea quarks since it is at large  $N_c$ . The recently discovered enhancement of initial-state interactions [26] is also expected to be most significant at small  $x$ , throwing into doubt the simple connection between light-cone probabilities and the Drell-Yan cross-section [27]. It is obviously desirable to have data on  $V_\pi$  from sources other than the Drell-Yan process. This is also important from the theoretical perspective, given that the current Dyson-Schwinger approach predicts a completely different shape for the pion distribution function [28].

## B. Distribution amplitude

The distribution amplitude (in  $A_- = 0$  gauge) for the pion is defined by

$$\langle 0 | \bar{\Psi}(z) \gamma^\mu \gamma_5 \Psi(0) | \psi_\pi(P^\mu) \rangle \Big|_{z^2=0} = f_\pi P^\mu \int_0^1 e^{ix(z \cdot P)} \phi_\pi(x) dx \quad (32)$$

with the normalisation condition

$$\int_0^1 \phi_\pi(x) = 1. \quad (33)$$

If the quark field correlator is to be evaluated at equal light-cone time,  $z^+ = 0$ , then  $\mathbf{z} = 0$  and  $z^-$  is arbitrary. This then measures the amplitude for zero transverse separation of quarks in the meson light-cone wavefunction. For the transverse lattice one finds

$$\psi_{+-}(x, 1-x) = \frac{f_\pi}{2} \sqrt{\frac{\pi}{N_c}} \phi_\pi(x) \quad (34)$$

from the  $\gamma^+$  component of (32). Fig. 8 shows our results for the distribution amplitude at various  $K$  and extrapolated to  $K = \infty$  in a three-link truncation. The raw (discrete) DLCQ data has been fit at each  $K$  to the first few terms of the conformal expansion [29, 30]

$$\phi_\pi(x) = 6x(1-x) \left\{ 1 + a_2 C_2^{3/2}(1-2x) + a_4 C_4^{3/2}(1-2x) \right\} . \quad (35)$$

An extrapolation of the coefficients with  $A + B/K + C/K^2$  yields  $a_2 = 0.15(2)$ ,  $a_4 = 0.04(1)$ , confirming that truncation of the conformal expansion is justified. The same values are obtained if the fit curves at each  $K$  are pointwise extrapolated and then refit to (35). Finally, the result is insensitive to whether the  $x = 1/2K$  and  $x = 1 - 1/2K$  endpoints are included in the fit or not, so we have shown them in Fig. 8 also.

The distribution amplitude is indirectly accessible through the pion transition form factor  $F_{\pi\gamma^*\gamma}(Q^2)$  measured at CLEO [31]. A perturbative QCD analysis relates this to the inverse moment, up to radiative corrections  $\Delta$ ,

$$\frac{3Q^2}{4\pi} F_{\gamma^*\gamma\pi} = \int_0^1 \frac{\phi_\pi(x)}{x} + \Delta = 3(1 + a_2 + a_4) + \Delta \quad (36)$$

An analysis of the data in Ref. [32] extracted  $a_2 + a_4 = 0.05 \pm 0.07$  at scale 2.4 GeV, taking into account next-to-leading order corrections  $O(\alpha_s)$  in  $\Delta$ . If we assume, following the structure function analysis, a scale 0.5 GeV for the transverse lattice result, when evolved to 2.4 GeV by the 1-loop evolution equations we find  $a_2 = 0.07(1)$ ,  $a_4 = 0.01(1)$  including only DLCQ errors. Although our result seems consistent with experiment, a couple of comments are necessary. The inverse moment is highly sensitive to the endpoint regions of  $\phi_\pi$ , which are not well covered by the extrapolation of the DLCQ transverse lattice result. Also, the leading radiative corrections in  $\Delta$  are large  $\sim 20\%$ , so one might ask about higher order corrections. The reader is referred to refs.[16, 33] for a more detailed review of the various theoretical and experimental results relating to  $\phi_\pi$ .

Diffraction dissociation on a nucleus  $\pi + A \rightarrow A + \text{jets}$  [34] has been used to measure a cross-section related to  $\phi_\pi$ . A number of theoretical analyses of that relation have recently been performed [35], which differ in their conclusions about the precise relationship. Our result, when evolved to the higher transverse momentum scale of the experiments, is consistent with any one of the analyses, being close to the asymptotic form  $6x(1-x)$ . We mention that our DLCQ transverse lattice result for  $\phi_\pi$  is close to one previously obtained in a one-link truncation using very similar methods [8], although  $a_4$  was not fit and the normalisation  $f_\pi$  was completely wrong in that case. The same 1-link truncation was investigated in Ref. [9] by using basis functions instead of DLCQ and a similar (but not identical) criteria for fixing the Hamiltonian couplings. That gave a distribution amplitude a little closer to the asymptotic form, although a value for  $a_2$  was not extracted and no error estimate was given. Thus, we can say with some confidence that our result is neither the ‘double-hump’ first found by Chernyak and Zhitnitsky [19] using (local) sum rules nor the ‘narrow-hump’ one would deduce from the latest Euclidean lattice measurements of the lowest moment of  $\phi_\pi$  [36].

### C. Quark helicity correlation

Although the pion is spin 0, it nevertheless contains a complicated spin structure. One measure of this is the quark helicity correlations

$$C^{\text{para}}(x) = \sum_h |\psi_{hh}(x, 1-x)|^2 + \sum_\lambda \sum_h \int_0^{1-x} dy |\psi_{h(\lambda)h}(x, y, 1-x-y)|^2 \\ + \sum_{\lambda, \rho} \sum_h \int_0^{1-x} dy \int_0^{1-x-y} dz |\psi_{h(\lambda\rho)h}(x, y, z, 1-x-y-z)|^2 + \dots, \quad (37)$$

$$C^{\text{anti}}(x) = \sum_h |\psi_{-hh}(x, 1-x)|^2 + \sum_\lambda \sum_h \int_0^{1-x} dy |\psi_{-h(\lambda)h}(x, y, 1-x-y)|^2 \\ + \sum_{\lambda, \rho} \sum_h \int_0^{1-x} dy \int_0^{1-x-y} dz |\psi_{-h(\lambda\rho)h}(x, y, z, 1-x-y-z)|^2 + \dots. \quad (38)$$

They measure the probability for a quark to have light-cone momentum fraction  $x$  and helicity either parallel or anti-parallel to that of the anti-quark. Therefore their sum is normalised to one (when integrated over  $x$ ). These functions are plotted in Fig. 9 for the pion. Although different from one another in the bulk of  $x$ , both  $C_\pi^{\text{para}}(x)$  and  $C_\pi^{\text{anti}}(x)$  have exponents  $\alpha$  and  $\beta$  consistent within errors with those of  $V_\pi(x)$  (see Fig. 6). We estimate that

$$\int_0^1 C_\pi^{\text{para}} dx \sim 0.45. \quad (39)$$

Therefore, one is almost equally likely to find quark helicities aligned as anti-aligned!

## V. CONCLUSIONS

We have extended coarse transverse lattice calculations to physically realistic cut-offs on the anti-quark—quark separation. A general light-cone hamiltonian in the large  $N_c$  limit was expanded in powers of dynamical fields and we studied a truncation of that colour-dielectric expansion. This included all possible cubic terms and most of the quartic terms. By optimising Lorentz covariance of glueball, heavy-source and meson boundstates, the remaining freedom in the couplings in the Hamiltonian was reduced. By studying other symmetries, such as parity and chirality, it may be possible to constrain them further. In this paper, we performed a phenomenological calculation by fixing the remaining freedom in the couplings to best fit  $\sqrt{\sigma}$ ,  $\mathcal{M}_\pi$ ,  $\mathcal{M}_\rho$ , and  $f_\pi$  (two of these are parameters of first-principles QCD).

The lightest meson bound state has the quantum numbers of the pion and exhibits a reasonably covariant lightcone wavefunction. Comparing the predictions of this wavefunction with various experimentally measured observables for the pion, we find consistency in the regions insensitive to sea quarks. New observables, which in principle can be extracted from a higher twist analysis of experiments, follow from the multi-parton correlations in the light-cone wavefunction. As an example, we computed the anti-quark—quark helicity correlation, with somewhat surprising results. Because the tail of the pion wavefunction is still truncated in our calculation, we did not compute observables sensitive to small transverse momentum. Nevertheless, it would be interesting to look at the general features of the skewed parton

distributions for intermediate momentum transfers, since little hard information is available for these important observables. It should be straightforward to extend the calculations to strange mesons and heavy-light mesons.

There are still some shortcomings in the calculation. The rho boundstate is not yet behaving covariantly. Our optimization of chiral symmetry could be considerably improved. Given the close connection of Lorentz and chiral symmetry on the lattice, we believe that these problems are related. In particular, higher-order terms in the colour-dielectric expansion can fulfill a dual role to improve both these symmetries.

Acknowledgements: The work of SD was supported in part by PPARC grant GR/LO3965. BvdS was supported by an award from Research Corporation. We would like to thank Geneva College undergraduates E. M. Watson and J. Bratt for help with developing the numerical code.

## APPENDIX: Chiral symmetry

The lattice Lagrangian (3) explicitly breaks chiral symmetry

$$\Psi \rightarrow e^{-i\theta\gamma_5}\Psi, \quad (40)$$

through the bare mass-term  $\mu_f$  and Wilson term  $\kappa_s$ . The standard test for this at the hadron level is PCAC

$$\langle 0 | \partial_\mu A^\mu | \psi_\pi \rangle = f_\pi \mathcal{M}_\pi^2, \quad (41)$$

where  $A_\mu$  is the axial current. Without knowing the precise form of  $A_\mu$ , one can use  $\mathcal{M}_\pi$  to quantify the amount of explicit chiral symmetry breaking relative to other scales, such as the pure-QCD mass gap or the spontaneous chiral symmetry breaking scale given by the difference between  $\mathcal{M}_\pi$  and masses of other light mesons. The result (41) relies on exact Lorentz covariance, which is not present on the transverse lattice. In fact, in the calculation performed in this paper, the splitting of the  $\rho$  Lorentz multiplet is of comparable strength to the  $\pi$ - $\rho$  splitting. This suggests that explicit chiral symmetry breaking effects are larger than  $\mathcal{M}_\pi$  would suggest, perhaps of the same order as spontaneous chiral symmetry breaking effects.

Explicit chiral symmetry breaking could in principle be tested more directly. There is a 1 + 1-dimensional Noether ‘vector’ current

$$j^\alpha = \sum_{\mathbf{x}} \bar{\Psi}(\mathbf{x}) \gamma^\alpha \Psi(\mathbf{x}) \quad (42)$$

that is conserved under the equations of motion, i.e.  $\partial_\alpha j^\alpha = 0$ , and a corresponding chiral current

$$j_5^\alpha = \sum_{\mathbf{x}} \bar{\Psi}(\mathbf{x}) \gamma^\alpha \gamma_5 \Psi(\mathbf{x}) \quad (43)$$

for which we find

$$\partial_\alpha j_5^\alpha = 2\mu_f^2 \sum_{\mathbf{x},h} h F_h^\dagger(\mathbf{x}) \frac{1}{\partial_-} F_h(\mathbf{x}). \quad (44)$$



where  $F_h$  is defined in eq. (8). One might then use a matrix element such as

$$\langle 0 | \partial_\alpha j_5^\alpha | \psi_\pi \rangle \quad (45)$$

to quantify explicit chiral symmetry violation, minimizing it by finite renormalisations of couplings, since the vanishing of (45) is a necessary condition for conservation of the four-dimensional axial current. There are a few difficulties that must be overcome before this would be practical however. The expression (44) has a normal-ordering ambiguity similar to the hamiltonian. Moreover, it is much more computationally expensive to perform symmetry tests with eigenfunctions rather than eigenvalues. On a coarse lattice, the chiral symmetry breaking couplings are also strongly constrained away from zero by Lorentz covariance; for example,  $\kappa_s$  is needed to avoid fermion doubling [7]. It would therefore be desirable to have further independent chiral symmetry breaking couplings in the theory to tune.

Natural candidates are the transverse lattice versions of the Sheikholeslami-Wohlert terms [37],  $\bar{\Psi} \sigma^{\mu\nu} F_{\mu\nu} \Psi$ , that can be used in Euclidean lattice gauge theory to remove  $O(a)$  contributions to chiral current non-conservation [38]. They become

$$\bar{\Psi}(\mathbf{x}) \sigma^{rs} (M_r(\mathbf{x}) M_s(\mathbf{x} + a\hat{r}) - M_s(\mathbf{x}) M_r(\mathbf{x} + a\hat{s})) \Psi(\mathbf{x} + a\hat{r} + a\hat{s}) , \quad (46)$$

$$\bar{\Psi}(\mathbf{x}) \sigma^{+-} F_{+-} \Psi(\mathbf{x}) \quad (47)$$

While in the dimensional counting classification of Euclidean lattice operators they occur along with Wilson terms at dimension five, on the coarse transverse lattice their significance is not so obvious since they contribute to higher orders of the colour-dielectric expansion. Terms of the form (46)(47) in the Lagrangian give rise to coupled constraint equations of motion for non-dynamical fields. If solved order by order in dynamical fields, they give rise to new interactions in the gauge-fixed light-cone hamiltonian starting at order  $u^4$ ,  $u^2 M^2$ . Of particular interest are interactions generated at order  $u^2 M^3$  and  $u^4 M$  that flip the helicity  $h$  of quarks. Such interactions carry the spontaneous chiral symmetry breaking effects in effective light-cone hamiltonians [39]; the  $m_f k_a$  and  $k_s k_a$  terms performed this function in (26).

- 
- [1] S. J. Brodsky, Acta Phys. Polon. B **32**, 4013 (2001);  
S. J. Brodsky, H.-C. Pauli, and S. Pinsky, Phys. Rep. **301**, 299 (1998).
  - [2] W. A. Bardeen and R. B. Pearson, Phys. Rev. D **14**, 547 (1976);  
W. A. Bardeen, R. B. Pearson, and E. Rabinovici, Phys. Rev. D **21**, 1037 (1980).
  - [3] M. Burkardt and S. Dalley, Prog. Part. Nucl. Phys. **48**, 317 (2002).
  - [4] P. A. Griffin, Nucl. Phys. B **139**, 270 (1992).
  - [5] S. Dalley and B. van de Sande, Phys. Rev. D **56**, 7917 (1997); Phys. Rev. D **59**, 065008 (1999);  
Phys. Rev. Lett. **82**, 1088 (1999); Phys. Rev. D **62**, 014507 (2000); Phys. Rev. D **63**, 076004 (2001).

- [6] M. Burkardt and B. Klindworth, Phys. Rev. D **55**, 1001 (1997).
- [7] M. Burkardt and H. El-Khozondar, Phys. Rev. D **60**, 054504 (1999).
- [8] S. Dalley, Phys. Rev. D **64**, 036006 (2001)
- [9] M. Burkardt and S. K. Seal, Phys. Rev. D **64**, 111501 (2001); Phys. Rev. D **65**, 034501 (2002).
- [10] H.-C. Pauli and S. J. Brodsky, Phys. Rev. D **32**, 1993 (1985); *ibid* 2001.
- [11] A. Casher, Phys. Rev. D **14**, 452 (1976);  
T. Maskawa and K. Yamawaki, Prog. Theor. Phys. **56**, 270 (1976).  
C. Thorn, Phys. Lett. B **70**, 77 (1977).
- [12] F. Antonuccio and S. Dalley, Phys. Lett. B **376**, 154 (1996); Nucl. Phys. B **461**, 275 (1996).
- [13] G. 't Hooft, Nucl. Phys. B **75**, 461 (1974).
- [14] M. Burkardt, Phys. Rev. D **57**, 1136 (1998).
- [15] A. Harindranath and R. Perry, Phys. Rev. D **43**, 4051 (1991).
- [16] E. Ruiz Arriola, Lectures at 42nd Cracow School of Theoretical Physics, Zakopane, Poland,  
31 May – 9 Jun 2002, [hep-ph/0210007](#).
- [17] F. Antonuccio, S. J. Brodsky, and S. Dalley, Phys. Lett. B **412**, 104 (1997).
- [18] S. Capitani *et al.* [QCDSF Collaboration], Nucl. Phys. Proc. Suppl. **106**, 299 (2002),  
[hep-lat/0111012](#);  
C. Best *et al.*, Phys. Rev. D **56**, 2743 (1997).
- [19] V. L. Chernyak and A. R. Zhitnitsky, Phys. Rep. **112**, 173 (1984).
- [20] S. V. Mikhailov and A. V. Radyushkin, Phys. Rev. D **45**, 1754 (1992).
- [21] M. B. Hecht, C. D. Roberts, and S. M. Schmidt, Phys. Rev. C **63**, 025213 (2001).
- [22] P. J. Sutton *et al.*, Phys. Rev. D **45**, 2349 (1992).
- [23] J. S. Conway *et al.* [E615 Collaboration], Phys. Rev. D **39**, 92 (1989).
- [24] B. Betev *et al.* [NA10 Collaboration], Z. Phys. C **28**, 15 (1985).
- [25] J. Badier *et al.* [NA3 Collaboration], Z. Phys. C **18**, 281 (1983).
- [26] S. J. Brodsky *et al.*, Phys. Rev. D **65**, 114025 (2002).
- [27] S. D. Drell and T. M. Yan, Phys. Rev. Lett. **24**, 181 (1970).
- [28] C. D. Roberts, Nucl. Phys. Proc. Suppl. **108**, 227 (2002), [nucl-th/0111030](#).
- [29] G. P. Lepage and S. J. Brodsky, Phys. Lett. B **87**, 359 (1979); Phys. Rev. D **22**, 2157 (1980).
- [30] A. V. Efremov and A. V. Radyushkin, Phys. Lett. B **94**, 245 (1980); Theor. Math. Phys. **42**,  
97 (1980).

- [31] J. Gronberg *et al.* [CLEO Collaboration], Phys. Rev. D **57**, 33 (1998).
- [32] A. Schmedding and O. Yakovlev, Phys. Rev. D **62**, 116002 (2000).
- [33] A. P. Bakulev, S. V. Mikhailov, and N. G. Stefanis, Phys. Lett. B **508**, 279 (2001).
- [34] E. M. Aitala *et al.* [E791 Collaboration], Phys. Rev. Lett. **86**, 4768 (2001).
- [35] L. Frankfurt, G. A. Miller, and M. Strikman, Phys. Rev. D **65**, 094015 (2002);  
V. M. Braun, D. Yu. Ivanov, A. Schafer, and L. Szymanowski, Phys. Lett. B **509**, 43 (2001);  
Nucl. Phys. B **638**, 111 (2002).  
V.L. Chernyak and A. G. Grozin, Phys. Lett. B **517**, 119 (2001).
- [36] L. Del Debbio *et al.*, Nucl. Phys. B (Proc. Suppl.) **83**, 235 (2000).
- [37] B. Sheikholeslami and R. Wohlert, Nucl. Phys. B **259**, 572 (1985).
- [38] M. Lüscher *et al.*, Nucl. Phys. B (Proc. Suppl.) **53**, 905 (1997).
- [39] K. G. Wilson *et. al.*, Phys. Rev. D **49**, 6720 (1994).

$\frac{1}{x} \left( m_f^2 + \delta m_p^2 + \frac{(k_a^2 + k_s^2)}{\pi} \int_0^x \frac{dy}{y} \right)$	(i)
$\frac{1}{2\sqrt{\pi y}} \left( \frac{1}{x+y} - \frac{1}{x} \right) \left\{ m_f k_s + m_f k_a \text{Sgn}[\lambda] (\delta_{ \lambda 2} - i h \delta_{ \lambda 1}) \right\}$	(ii)
$\frac{-1}{2\pi} \text{P} \left( \frac{1}{(x-y)^2} \right)$	(iii)
$\frac{-(y-z)}{4\pi(y+z)^2 \sqrt{yz}} \delta_{-\lambda\rho}$	(iv)
$\frac{1}{4\pi(x+y)\sqrt{yz}} \left\{ k_s^2 \delta_{hh'} + k_a^2 \delta_{hh'} (\delta_{\lambda\rho} - \delta_{-\lambda\rho} - i h \text{Rot}[\lambda, \rho]) \right.$ $\left. + k_a k_s \delta_{-hh'} \left( \text{Sgn}[\lambda] (i h \delta_{ \lambda 1} - \delta_{ \lambda 2}) + \text{Sgn}[\rho] (i h \delta_{ \rho 1} - \delta_{ \rho 2}) \right) \right\}$	(v)
$\frac{1}{4\pi(x+y)\sqrt{yz}} \left\{ k_s^2 \delta_{hh'} + k_a^2 \delta_{hh'} (\delta_{-\lambda\rho} - \delta_{\lambda\rho} + i h \text{Rot}[\lambda, \rho]) \right.$ $\left. + k_a k_s \delta_{-hh'} \left( \text{Sgn}[\lambda] (i h \delta_{ \lambda 1} - \delta_{ \lambda 2}) - \text{Sgn}[\rho] (i h \delta_{ \rho 1} - \delta_{ \rho 2}) \right) \right\}$	(vi)
$\frac{m_b^2}{x}$	(vii)
$\frac{-1}{4\pi} \text{P} \left( \frac{y+z}{\sqrt{zy}(z-y)^2} \right)$	(viii)
$\frac{-1}{8\pi} \text{P} \left( \frac{(y+z)(2x+y-z)}{\sqrt{xzy}(x+y-z)(z-y)^2} \right)$	(ix)
$\frac{1}{4\pi\sqrt{xyz(x+z-y)}} \left\{ 2l_1 \delta_{\sigma\lambda} \delta_{\rho\tau} \delta_{-\rho\sigma} + l_2 (\delta_{\sigma\lambda} \delta_{\rho\tau} \delta_{\rho\sigma} + \delta_{-\sigma\rho} \delta_{-\lambda\tau} \delta_{-\sigma\lambda}) \right.$ $\left. + l_4 (\delta_{\sigma\lambda} \delta_{\rho\tau}  \text{Rot}[\sigma, \rho]  + \delta_{-\sigma\rho} \delta_{-\lambda\tau}  \text{Rot}[\sigma, \lambda] ) - b \delta_{\lambda\rho} \delta_{\sigma\tau}  \text{Rot}[\sigma, \rho]  \right\}$	(x)
$\frac{1}{4\pi\sqrt{xyz(x+z+y)}} \left\{ 2l_1 \delta_{-\sigma\lambda} \delta_{\lambda\tau} \delta_{\lambda\rho} + l_2 \delta_{\sigma\tau} \delta_{-\lambda\rho} \delta_{ \lambda  \sigma } \right.$ $\left. + l_4 (\delta_{-\lambda\sigma} \delta_{\rho\tau}  \text{Rot}[\lambda, \rho]  + \delta_{-\sigma\rho} \delta_{\lambda\tau}  \text{Rot}[\sigma, \lambda] ) - b \delta_{-\lambda\rho} \delta_{\sigma\tau}  \text{Rot}[\sigma, \lambda]  \right\}$	(xi)
$\frac{-1}{8\pi} \frac{(y-z)(2x+y+z)}{\sqrt{xzy}(x+y+z)(z+y)^2} \delta_{-\lambda\rho}$	(xii)
$\frac{-1}{8\pi} \frac{(x-z)(2y-x-z)}{\sqrt{xzy}(x-y+z)(z+x)^2} \delta_{-\sigma\rho} \delta_{-\lambda\tau}$	(xiii)

TABLE I: Matrix elements of the dimensionless invariant mass operator  $2P^+P^-/\bar{G}^2$  in Fock space.

Momentum conserving delta functions are omitted for clarity.

$m_b$	$b$	$l_1$	$l_2$	$l_4$	$k_s$	$k_a$	$m_f$	$\delta m_0^2$	$\delta m_1^2$	$\delta m_2^2$
0.276	0.768	-0.169	-0.186	0.024	0.420	0.652	0.236	1	-0.127	-0.035

TABLE II: Optimum coupling constants at  $a = 2/3$  fm for a three-link truncation. Note that  $\delta m_0^2$  was swept more coarsely than the other couplings.

State	Mass(MeV)	$c$
$\pi$	171	1.02
$\rho_0$	828	0.99
$\rho_+$	457	1.04
$\rho_-$	457	0.76

TABLE III: Meson dispersion at the optimum couplings.

#Links	0	1	2	3
Probability	0.097(14)	0.661(10)	0.150(8)	0.087(2)

TABLE IV: Probability for finding a certain number of links in the pion. The extrapolation errors in brackets are from a  $1/K$  extrapolation.

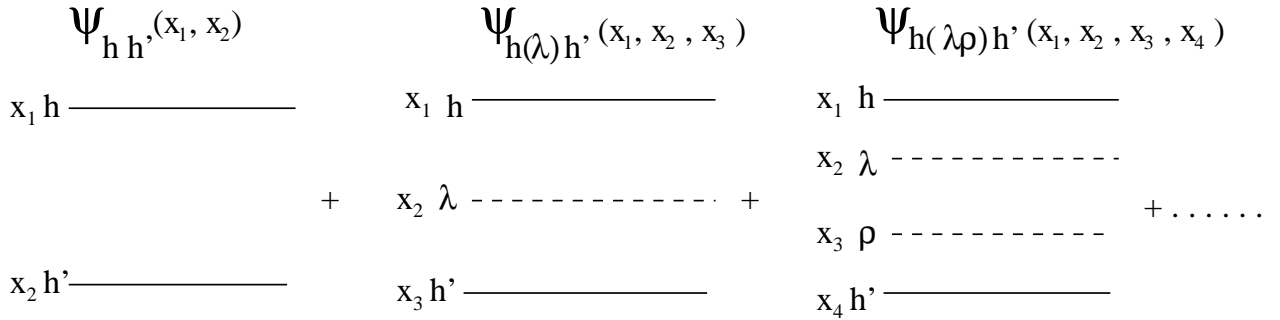


FIG. 1: Planar diagram representation of the Fock space structure of a meson boundstate. Solid lines represent quarks/anti-quarks, chain lines link fields.

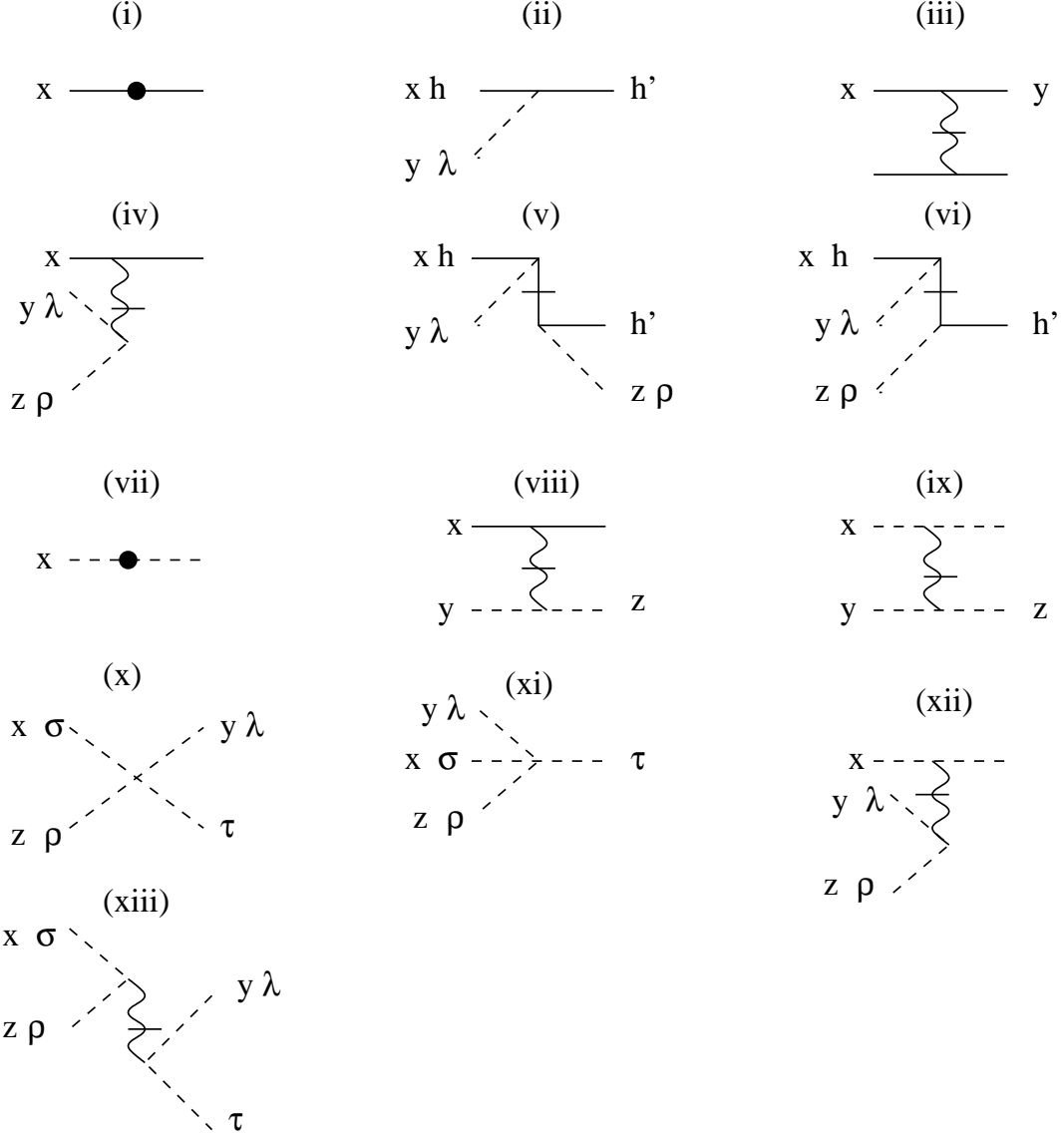


FIG. 2: Planar diagram representation of the elementary amplitudes contributing to (26). Vertical barred lines are  $x^+$ -instantaneous interactions.

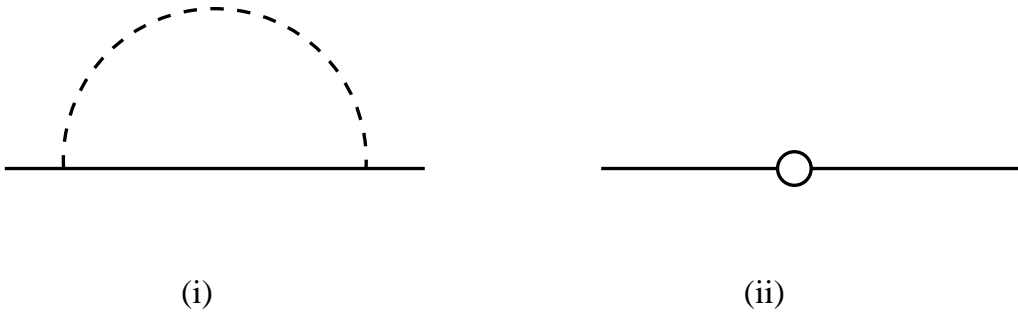


FIG. 3: (i) one-loop logarithmically divergent quark self-energy (ii) logarithmically divergent mass insertion counterterm represented by open circle .

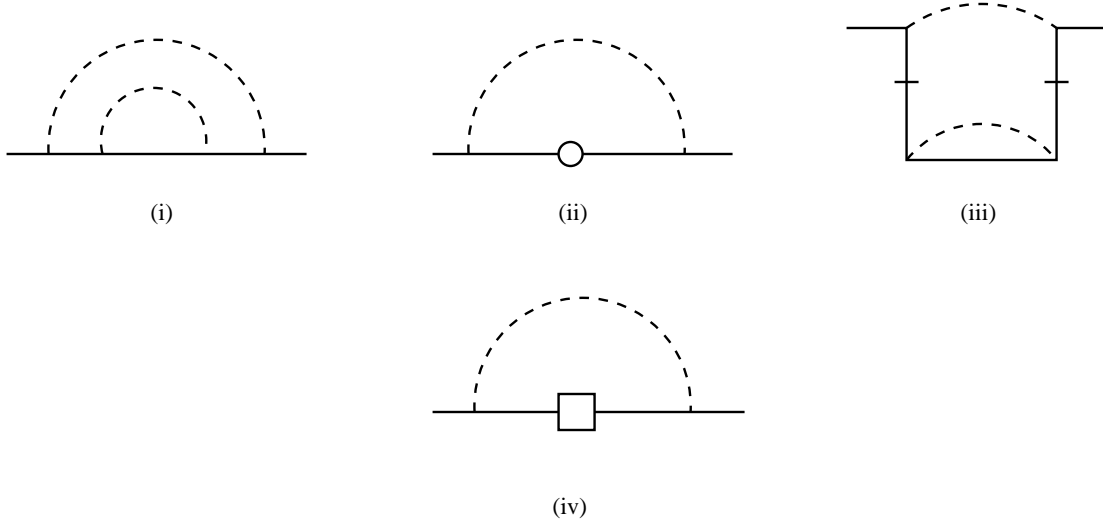


FIG. 4: (i)(iii) two-loop logarithmically divergent quark self-energies (ii) one-loop diagram with infinite mass insertion (iv) one-loop diagram with finite mass insertion  $\delta m^2$  represented by open box

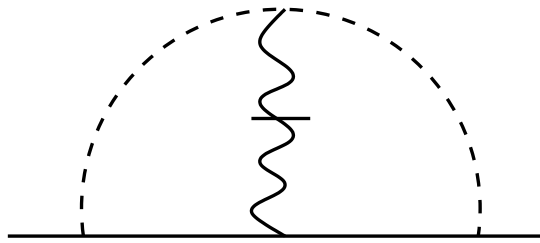


FIG. 5: Finite diagram with instantaneous interaction dressing

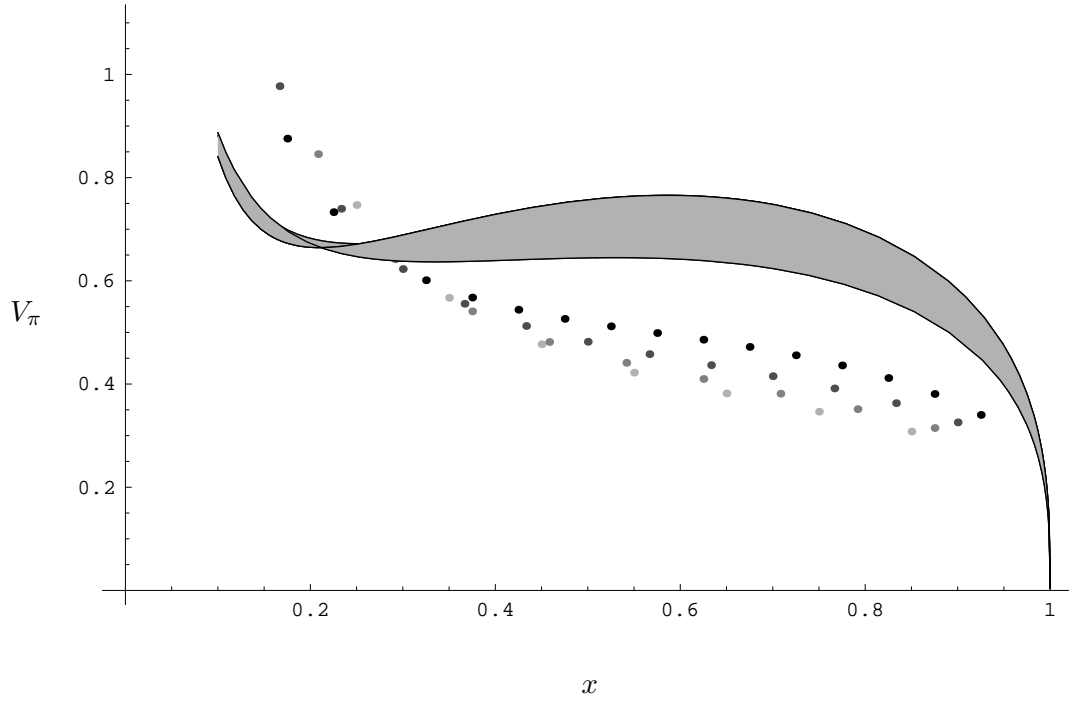


FIG. 6: Pion distribution function for DLCQ cutoffs  $K = 10, 12, 15, 20$ , darker data points meaning larger  $K$ .  $K \rightarrow \infty$  extrapolated curve lies in the shaded region.



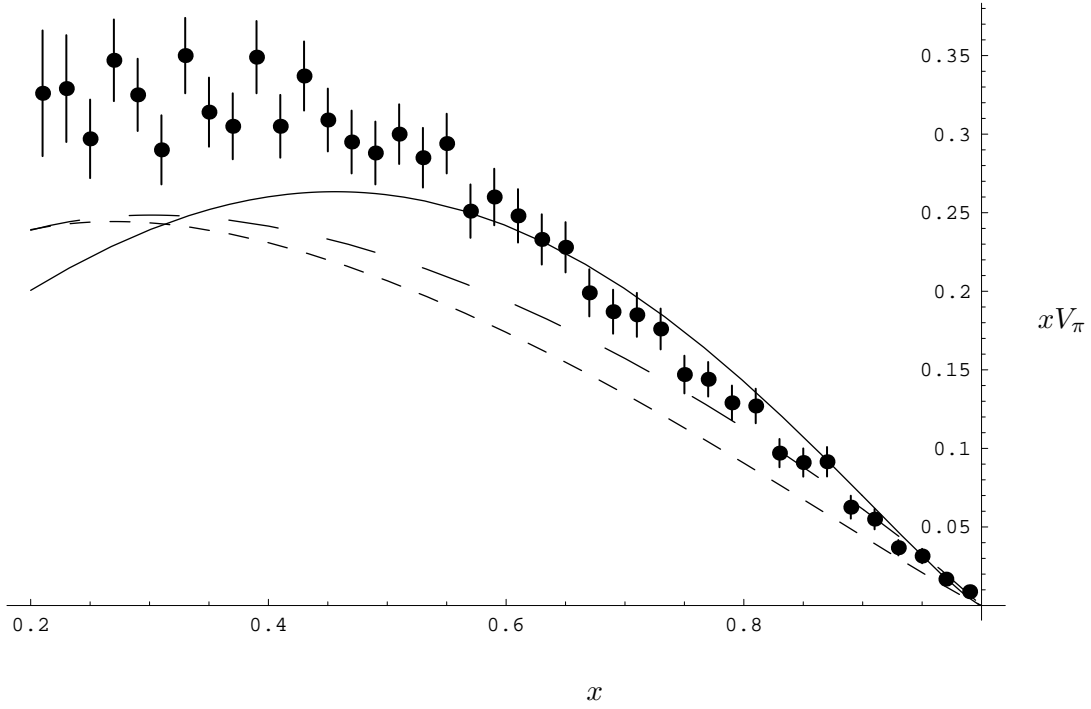


FIG. 7: Pion (valence) distribution function (times  $x$ ) compared to pion-nucleon Drell-Yan data. Solid line: transverse lattice result evolved to 6.6 GeV. Data points: E615 experiment. Short-dashed line: NA10 experiment fit to  $x^\alpha(1-x)^\beta$  form. Long-dashed line: NA3 experiment fit to  $x^\alpha(1-x)^\beta$  form.

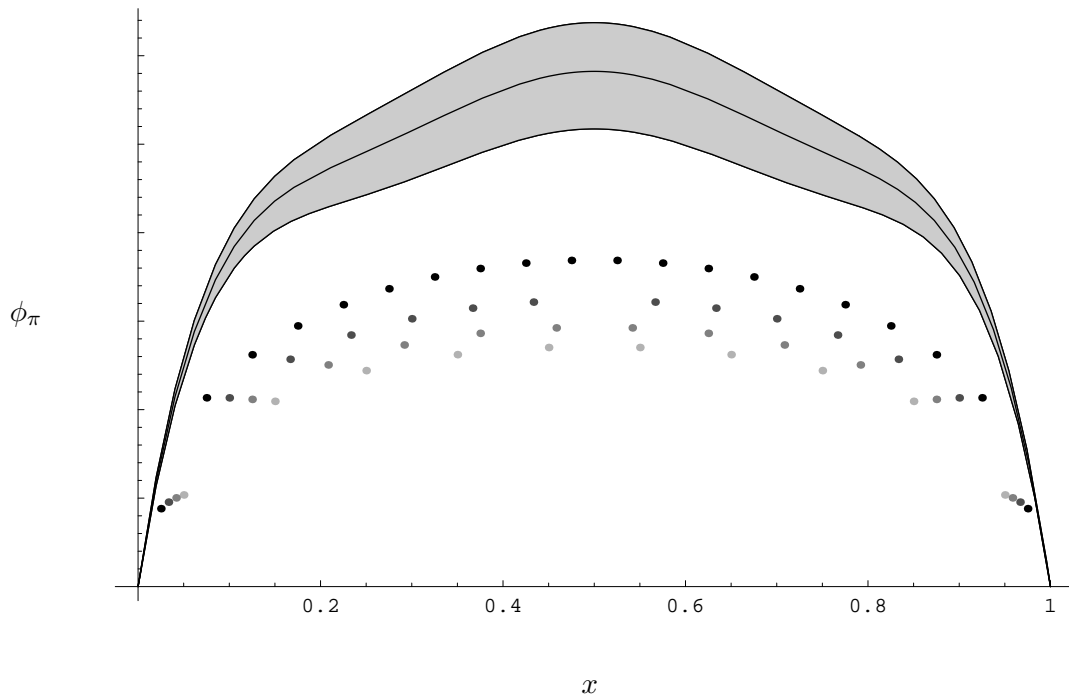


FIG. 8: Pion distribution amplitude for DLCQ cutoffs  $K = 10, 12, 15, 20$ , darker data points meaning larger  $K$ .  $K \rightarrow \infty$  extrapolated curve lies in the shaded region.

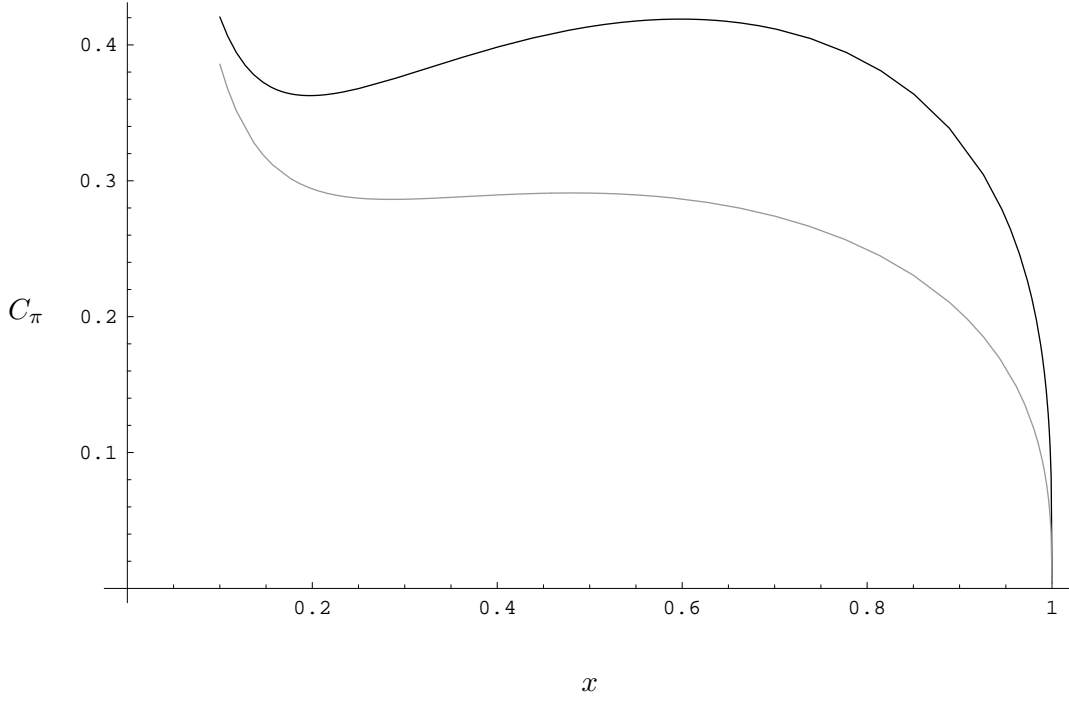


FIG. 9: Extrapolated quark helicity correlation function for the pion: black for anti-parallel helicities  $C_\pi^{\text{anti}}$ ; grey for parallel helicities  $C_\pi^{\text{para}}$ .